Mechanical Properties and Superstructure of High-Modulus and High-Strength PET Fiber Prepared by Zone Annealing

TOSHIO KUNUGI, AKIHIRO SUZUKI, and MINORU HASHIMOTO,
Department of Applied Chemistry, Faculty of Engineering, Yamanashi University, Kofu-shi, 400 Japan

Synopsis

The relationships between mechanical properties and superstructure of the poly(ethylene terephthalate) fiber prepared by a new annealing method called zone annealing method were investigated. The effectiveness of zone annealing was compared with three other annealing methods, namely, annealing under release, annealing at constant length, and annealing under tension. The very high modulus and strength of the zone-annealed fiber were directly attributed to the large number of tie molecules connecting the crystallites and to the high orientation of the amorphous region.

INTRODUCTION

We succeeded in preparing high-modulus and high-strength fiber from crystalline polymer already widely used by a new annealing method called zone annealing method. This method has so far[1] been applied to poly(ethylene terephthalate), nylon 6, polyethylene, and polypropylene. Although the apparatus is simple and the procedure easy, the resulting fibers exhibited excellent mechanical properties and dimensional stability at elevated temperatures. In the preceding report[2] we outlined this new method and discussed the application to poly(ethylene terephthalate) fiber.

In the present report, we deal with the results of subsequent detailed research on PET. In particular, the relationship between mechanical properties and superstructure of the zone-annealed fiber were compared with those of fibers prepared by three other annealing methods.

EXPERIMENTAL

Material

The original material used in the present study is as-spun poly(ethylene terephthalate) fiber of diameter 0.48 mm supplied by Toray Co. Ltd. The fiber has a birefringence of 0.3×10^{-3} and a crystallinity of 1.8%.

Zone Drawing and Zone Annealing

The zone annealing procedure consists of two stages—zone drawing and zone annealing. The zone drawing was done on the original as-spun fiber in order to produce a fiber with as high an orientation and as low a crystallinity as possible,

Journal of Applied Polymer Science, Vol. 26, 1951–1960 (1981)
 CCC 0021-8995/81/061951-10$01.00

whereas the zone annealing was subsequently carried out to convert the zone-drawn fiber into a fiber with high orientation and high crystallinity.

The apparatus and the practical procedure are as follows. The apparatus used here is the usual tensile tester partially reconstructed. A band heater 2 mm wide was attached to the movable crosshead. The temperature of the band heater can be held constant throughout the experimental period by a control system. The upper end of the fiber was fixed and the desired tension was applied to the lower end by weighting. The band heater can be moved up or down along the fiber axis at a moving speed chosen from 2, 4, 8, 10, 20, or 40 mm/min. In this study, zone drawing and zone annealing were performed under the most suitable conditions determined in the previous report,[2] as seen in Table I.

Other Annealing Methods

In order to elucidate the characteristic effectiveness of the zone annealing method, the fibers prepared by three other annealing methods were compared with the zone-annealed fiber. These methods are annealing under release, annealing at constant length, and annealing under tension (16 kg/mm^2). All these annealings were carried out at 200°C for 30 min in an air oven on the fibers which were already drawn up to five times at 90°C.

Since the tension during annealing, as a matter of course, increases in the above order, a comparative study of superstructure and mechanical properties of the fibers prepared by these methods can reveal the effects of the tension during annealing. On the other hand, a comparison of the fiber annealed under high tension with the zone-annealed fiber is useful in the difference between annealing on the whole fiber and annealing on only part of the fiber, because both annealings are done at the same temperature and under the same tension.

Measurements

The mechanical properties of the fibers thus prepared were measured with a tensile strength tester and a viscoelastometer. The tensile properties were determined at 23–25°C, RH 65%, on a monofilament 20 mm long. Young's modulus, tensile strength, and elongation at break were estimated from the stress–strain curves. The dynamic viscoelastic properties, storage modulus E', loss modulus E'', and loss tangent tan δ were measured at 110 Hz at a heating rate of 1.5°C/min on fibers 20 mm long. The measurements were carried out in two temperature ranges: from −150°C to room temperature and from room temperature to 250°C. The lower temperature measurements were performed

TABLE I
The Most Suitable Conditions for Zone Drawing and Zone Annealing

Conditions	Zone drawing	Zone annealing
Temperature of heating zone, °C	90	200
Moving speed of band heater, mm/min	40	10
Moving direction of band heater	up	up or down
Tension applied to fiber, kg/mm^2	0.3	16
Repetition, times	1	5

in a stream of dry air cooled with liquid nitrogen, and the higher temperature measurements in a stream of dry nitrogen gas.

The density of the fibers was measured at 25°C by a flotation method[4] using toluene–carbon tetrachloride mixtures. From the obtained density, the degree of crystallinity was calculated by the usual method using a crystal density[5] of 1.455 g/cm^3 and an amorphous density[5] of 1.335 g/cm^3.

The birefringence was measured with a polarizing microscope equipped with Bereck's compensator. Because the highly oriented PET fibers have a very high retardation,[4] X–Z planes of various thicknesses cut from a single crystal of quartz were used as an additional compensator.

The orientation factor of crystallites (f_c) was evaluated by the x-ray diffraction method.[4] As is well known, f_c is defined by the following equation:

$$f_c = 1/2\,(3\langle\cos^2\Phi_{c,z}\rangle - 1) \tag{1}$$

Where $\langle\cos^2\Phi_{c,z}\rangle$ represents the mean-square cosine of the angle between the c axis and the fiber axis (z) and can be calculated by the following equation derived from an application of the Wilchinsky method[6]:

$$\langle\cos^2\Phi_{c,z}\rangle = 1 - 0.3481\langle\cos^2\Phi_{100,z}\rangle - 0.7733\langle\cos^2\Phi_{\bar{1}10,z}\rangle - 0.8786\langle\cos^2\Phi_{010,z}\rangle \tag{2}$$

where the quantities $\langle\cos^2\Phi_{100,z}\rangle$, $\langle\cos^2\Phi_{\bar{1}10,z}\rangle$, and $\langle\cos^2\Phi_{010,z}\rangle$ can be graphically determined from the azimuthal intensity distributions of x-ray diffraction for the (100), ($\bar{1}$10), and (010) planes, respectively.

The x-ray intensities used here were previously corrected for polarization, absorption, background noise, and incoherent scattering and were then carefully separated from the amorphous contribution and overlapping components arising from the adjacent planes to obtain the real crystalline diffraction from each plane.

The orientation factor of the amorphous region (f_a) was evaluated by combining x-ray and optical birefringence data. Generally, the measured birefringence of a semicrystalline specimen with cylindrical symmetric orientation (Δ_t) can be represented by the additivity[7] of birefringences as follows:

$$\Delta_t = \Delta_c^0 f_c X_c + \Delta_a^0 f_a (1 - X_c) + \Delta_f \tag{3}$$

where Δ_c^0 and Δ_a^0 are the intrinsic birefringences of the crystal and the amorphous phase, X_c is the crystallinity, and Δ_f is the form birefringence. The Δ_f is usually small enough relative to the other terms to be neglected. If Δ_f is neglected, the f_a value can be calculated by the following equation:

$$f_a = \frac{\Delta_t - \Delta_c^0 f_c X_c}{\Delta_a^0 (1 - X_c)} \tag{4}$$

In the above calculations, Δ_c^0 was taken as 0.251 proposed by us,[4] whereas Δ_a^0 was taken as 0.230, which was calculated based on the assumption that the ratio of Δ_c^0 to Δ_a^0 is equal to the ratio of crystal density (1.455) to amorphous density (1.335 g/cm^3).

Further, IR spectra, DSC curves, and x-ray Laue photographs of the fibers were also examined.

TABLE II
Mechanical Properties of Fibers Prepared by Four Different Annealing Methods

Sample	Young's modulus, $\times 10^{-10}$ dyn/cm^2	Strength at break, kg/mm^2	Elongation at break, %
Fiber annealed under release	6.5	30.2	23.7
Fiber annealed at constant length	7.8	42.4	25.5
Fiber annealed under tension	12.7	61.7	12.7
Fiber zone annealed	19.4	84.6	5.9

RESULTS AND DISCUSSION

Mechanical Properties

The tensile properties of the fibers prepared by the four kinds of annealing methods are compared in Table II. From the table, it can be seen that Young's modulus and strength at break increase, whereas elongation at break decreases, in the order of the fiber annealed under release, one annealed at constant length, one annealed under tension, and one zone annealed. This fact indicates that these properties can be improved by increasing the tension during annealing and that the annealing at a narrow zone of the fiber is far more effective than that over the whole fiber. Young's modulus of the zone-annealed fiber is significantly higher than those of fibers annealed in the other ways and corresponds to about 18% of the crystal modulus[8] along the molecular chains, 107.8×10^{10} dyn/cm^2.

Figures 1 and 2 show the temperature dependences of the dynamic storage modulus (E') in the two temperature ranges—one from room temperature to 250°C and the other from −150°C to room temperature, respectively. The E' value of the zone-annealed fiber is again highest over the whole temperature range. The magnitude of E' increases progressively in the same order as that of Young's modulus or the tensile strength. It can be said from these comparisons that the zone annealing method is most effective for improvement of the mechanical properties in spite of shifting the narrow heating zone and short heating time.

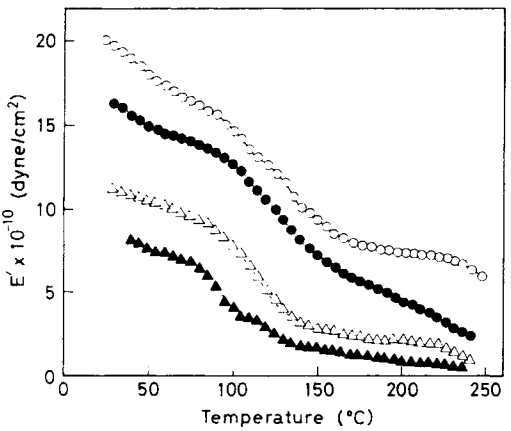

Fig. 1. Temperature dependence of dynamic modulus E' in the higher-temperature range for fibers prepared by four different annealing methods: (▲) fiber annealed under release; (△) fiber annealed at constant length; (●) fiber annealed under tension; (○) fiber zone annealed.

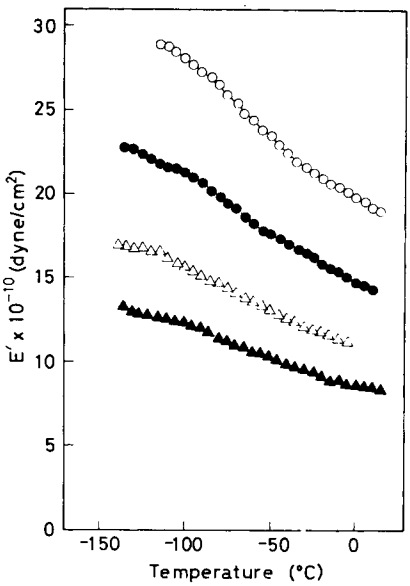

Fig. 2. Temperature dependence of dynamic modulus E' in the lower-temperature range for fibers prepared by four different annealing methods: (▲) fiber annealed under release; (△) fiber annealed at constant length; (●) fiber annealed under tension; (○) fiber zone annealed.

Orientation and Crystallinity

Table III shows the birefringence, orientation factors of crystalline and amorphous regions, and crystallinity for the four kinds of fibers. The values of all the orientation factors are arranged in the same order as in the case of the mechanical properties. This tendency also can be clearly seen in x-ray Laue photographs shown in Figure 3, in which each crystal plane reflection becomes narrow from arc to spot in the same order. Closer examination of Table III shows that, although the f_c values are fairly high for all the fibers and are close to each other, the birefringence and f_a increase remarkably and roughly in the same order. This suggests that the orientation, especially the orientation of amorphous chains, plays an important role in the improvement of the mechanical properties. The birefringence value of the zone-annealed fiber reached 0.247, which is higher than most[9–14] of the crystalline intrinsic birefringence values previously reported.

The magnitude of the crystallinity on the other hand, is not directly related to the mechanical properties. Although the fiber annealed under release has a fairly high degree of crystallinity, Young's modulus and the tensile strength

TABLE III
Orientation and Crystallinity of Fibers Prepared by Four Different Annealing Methods

Sample	Birefringence, $\times 10^3$	f_c	f_a	Crystallinity, %
Fiber annealed under release	185.4	0.964	0.573	52.1
Fiber annealed at constant length	202.9	0.979	0.787	40.5
Fiber annealed under tension	218.5	0.985	0.872	51.9
Fiber zone annealed	247.3	0.986	0.947	60.0

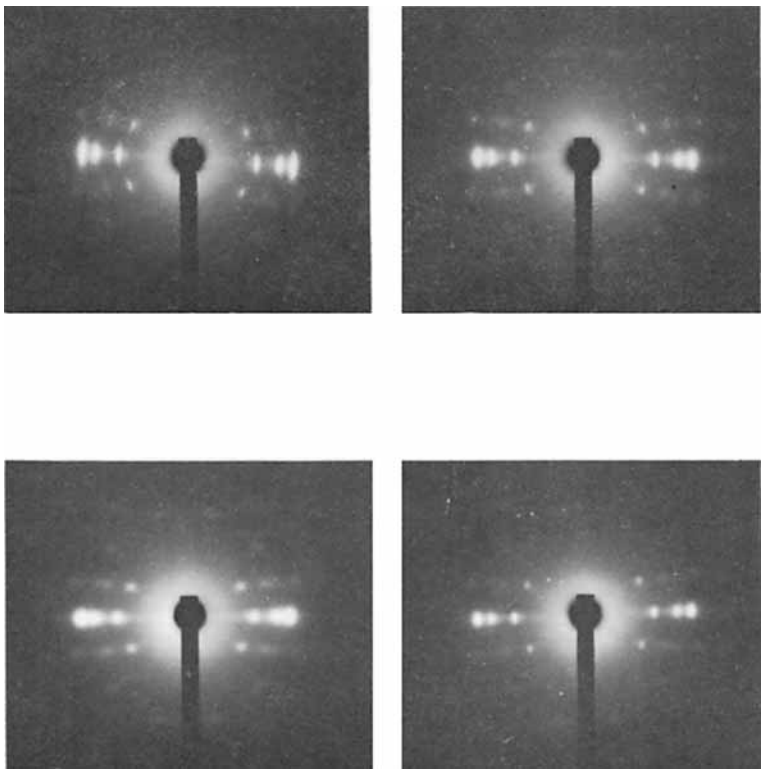

Fig. 3. X-Ray Laue photographs of fibers prepared by four different annealing methods.

of the fiber are only 33 and 35% of those of the zone-annealed fiber, respectively. This indicates that the crystalline portion of the fiber annealed under release consists of lamellae which are not very useful in transmitting the force.

Mechanical Dispersion Peaks and IR Spectra

Figures 4, 5, 6, and 7 show the temperature dependences of tan δ and loss modulus E'' in the two temperature ranges. Two large dispersion peaks ap-

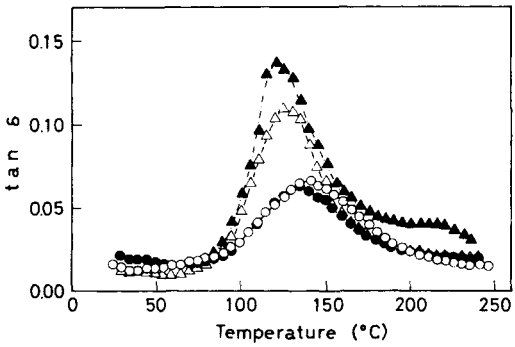

Fig. 4. Temperature dependence of loss tangent, tan δ, in the higher-temperature range for fibers prepared by four different annealing methods: (▲) fiber annealed under release; (△) fiber annealed at constant length; (●) fiber annealed under tension; (○) fiber zone annealed.

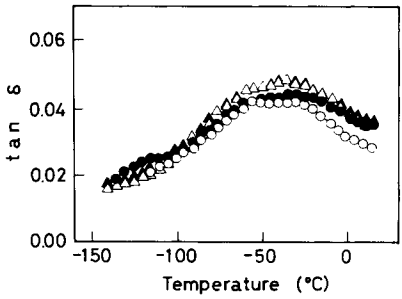

Fig. 5. Temperature dependence of loss tangent, tan δ, in the lower-temperature range for fibers prepared by four different annealing methods: (▲) fiber annealed under release; (△) fiber annealed at constant length; (●) fiber annealed under tension; (○) fiber zone annealed.

peared at 120–140°C and about −40°C in the tan δ–temperature curves, in contrast to 110–130°C and about −60°C in the E''–temperature curves. As is well known, the peak at the lower temperature corresponds to the β-dispersion peak,[15] whereas the peak at the higher temperature is the α-dispersion peak[15] ascribed to micro-Brownian motion of amorphous chains.

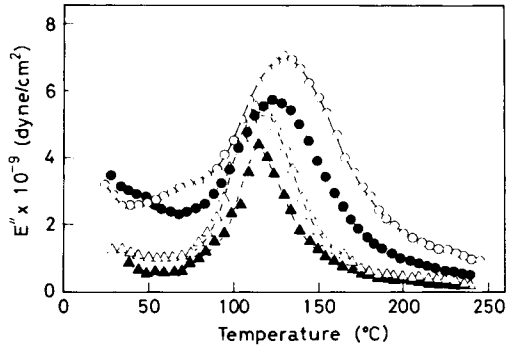

Fig. 6. Temperature dependence of loss modulus E'' in the higher-temperature range for the fibers prepared by four different annealing methods: (▲) fiber annealed under release; (△) fiber annealed at constant length; (●) fiber annealed under tension; (○) fiber zone annealed.

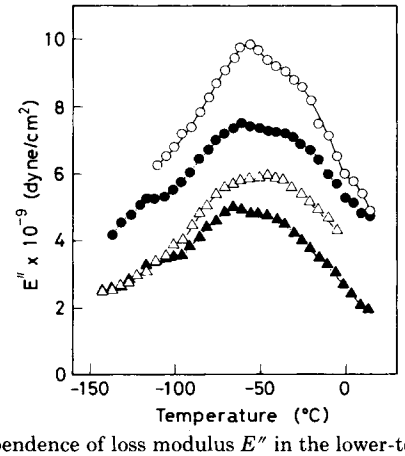

Fig. 7. Temperature dependence of loss modulus E'' in the lower-temperature range for fibers prepared by four different annealing methods: (▲) fiber annealed under release; (△) fiber annealed at constant length; (●) fiber annealed under tension; (○) fiber zone annealed.

From Figure 4, it is found that the α-dispersion peak becomes progressively smaller and broader and shifts to a higher temperature in the order described above. The temperature positions of the peaks for the four fibers are also listed in Table IV. This behavior of the α-dispersion peak indicates that the movement of the amorphous molecular chains at that temperature becomes progressively difficult in the same order. However, the intensity and its temperature position of the β-dispersion peak are virtually unaffected by the differences in the annealing methods, as seen in Figure 5.

In general, the behavior of the α-dispersion peak of a semicrystalline polymer is far more sensitive to the variation in the superstructures, compared with the β-dispersion peak. This fact was already reported by us[16] for nylon 6 fiber. As the motional units of segments related to a dispersion are larger, the dispersion is more strongly affected by the differences in the superstructures, which depend on the history of the fiber under consideration.

On the other hand, the intensities of the E'' peaks of both the α- and β-dispersions increase regularly in the same order, as seen in Figures 6 and 7. Because the intensity of the E'' dispersion peak[16] indicates the energy dissipated as frictional heat per cycle in a sinusoidal deformation, the increases in the peak intensities imply increases in intermolecular friction. From these observations, it can be assumed that the movement of the amorphous molecular chains of the zone-annealed fiber is significantly small compared with that in other fibers.

Further, the conformation of molecular chains was checked by IR measurements. Table V shows the relative intensities of IR absorption peaks arising from trans and gauche conformations for the four kinds of fibers. Here, the relative intensities[17] of both conformational bands are determined by dividing by the internal thickness band at 795 cm^{-1} to compare samples of various thickness on the same basis. It is clear from Table V that the trans conformation content increases and the gauche content decreases in the same order. It was also found that the 988 cm^{-1} absorption band assigned to a folded-chain con-

TABLE IV
Temperature of α-Dispersion Peak in tan δ–Temperature Curves for Fibers Prepared by Four Different Annealing Methods

Sample	Peak temperature, °C
Fiber annealed under release	120
Fiber annealed at constant length	125
Fiber annealed under tension	135
Fiber zone annealed	140

TABLE V
Conformations of Molecular Chains of Fibers Prepared by Four Different Annealing Methods

Sample	Trans conformation A_{973}/A_{795}	Gauche conformation A_{895}/A_{795}
Fiber annealed under release	1.25	0.89
Fiber annealed at constant length	1.67	0.83
Fiber annealed under tension	1.74	0.72
Fiber zone annealed	2.33	0.68

formation becomes gradually smaller in the same order from an isolated weak peak of the fiber annealed under release to a very weak shoulderlike peak of the zone-annealed fiber. On the basis of these experimental results, we assumed that the amorphous region of the zone-annealed fiber consisted of highly oriented and densely aggregated extended molecular bundles. The assumption is also supported by the excellent dimensional stability at elevated temperatures and the small-angle x-ray scattering feature of the zone-annealed fiber reported in the preceding article.[2]

Estimation of Amorphous Modulus and Number andFraction of Tie Molecules

Unless the crystalline region is completely continuous along the fiber axis, the amorphous region having a lower modulus has a more pronounced influence on the mechanical properties of the fiber than that of the crystalline region. In particular, the orientation of amorphous chains, the number and fraction of tie molecules, and the distribution of length and strain of tie molecules may be considered important factors concerning the amorphous region.

If a uniaxially oriented fiber can be represented by a mechanical structural model in which the crystalline and amorphous regions are arranged alternately in the fiber axis direction, the following equation can be used for additivity of compliances:[18]

$$\frac{1}{E_{\parallel}} = \frac{X_c}{E_{c\parallel}} + \frac{1 - X_c}{E_a} \tag{5}$$

where $E_{\parallel}$ is the as-measured macromodulus, $E_{c\parallel}$ is the crystal modulus along the molecular chains, and X_c is the volume crystallinity. When $E_{c\parallel} = 107.8 \times 10^{10}$ dyn/cm^2 and the measured X_c and $E_{\parallel}$ are substituted in the above equation, the amorphous modulus (E_a) for the fiber is given. This evaluation of E_a is based on the idea that, even when some fibers have the same value of crystallinity, each fiber may possess a different E_a value, its magnitude depending on individual superstructure.

The values of E_a thus calculated are listed in Table VI. The value of E_a also increases in the same order as in the case of Young's modulus, the strength at break, and the dynamic storage modulus. In particular, it should be noted that the increasing ratio of E_a to the E_a value of the fiber annealed under release is in fair agreement with that of Young's modulus. For example, in the case of the zone-annealed fiber, E_a is increased by 2.72, while Young's modulus increases

TABLE VI
Amorphous Modulus (E_a) and Number and Fraction of the Tie Molecules [$(1 - X_c)E/E_{c\parallel}$ and β_E] of Fibers Prepared by Four Different Annealing Methods

Sample	E_a, $\times 10^{-10}$ dyn/cm^2	$(1 - X_c)E/E_{c\parallel}$	β_E
Fiber annealed under release	3.2	0.029	0.060
Fiber annealed at constant length	4.8	0.043	0.072
Fiber annealed under tension	6.5	0.057	0.118
Fiber zone annealed	8.7	0.072	0.180

by 2.98 times those of the fiber annealed under release. It is obvious that the discrepancies in the mechanical properties among the four fibers arise from mainly those of the amorphous region.

Subsequently, the number and fraction of tie molecules were estimated by Peterlin's procedure.[19] Under the assumption that the elastic modulus is exclusively caused by tie molecules and that the tie molecules are uniformly distributed and all of equal length, he stated that the number and the fraction of tie molecules could be represented by $(1 - X_c)E_{\parallel}/E_{c\parallel}$ and $\beta_E = E_{\parallel}/E_{c\parallel}$, respectively. The obtained values of $(1 - X_c)E_{\parallel}/E_{c\parallel}$ and β_E are listed in Table VI. These values are also arranged in the same order of increasing magnitude as obtained for Young's modulus, strength at break, dynamic storage modulus, birefringence, f_a, and E_a.

Although these values are only a measure of the number of tie molecules, because the tie molecules in an actual fiber are of unequal length and are nonuniformly strained upon loading, it is certain that the zone-annealed fiber contains a large number of tie molecules. The large number of tie molecules contributes to the increase in E_a, and then the increase in E_a results in an increase in Young's modulus and strength of the whole fiber.

It can be concluded that the zone annealing procedure, particularly the high tension during annealing[20,21] and the slow moving of the narrow heating zone, is effective for the formation of an extended-chain structure, and consequently the obtained fiber exhibits excellent mechanical properties.

References

1. T. Kunugi, A. Suzuki, I. Akiyama, and M. Hashimoto, *Polym. Prepr. Am. Chem. Soc. Div. Polym. Chem.*, **20,** 778 (1979).
2. T. Kunugi, A. Suzuki, and M. Hashimoto, *J. Appl. Polym. Sci.*, **26,** 213 (1981).
3. T. Kunugi, *Sen i Gakkaishi*, **36,** P-411 (1980).
4. T. Kunugi, K. Shiratori, K. Uematsu, and M. Hashimoto, *Polymer*, **20,** 171 (1979).
5. S. Okajima and K. Kayama, *Sen i Gakkaishi*, **22,** 51 (1966).
6. Z. W. Wilchinsky, *J. Appl. Phys.*, **30,** 792 (1959).
7. R. S. Stein and F. H. Norris, *J. Polym. Sci.*, **21,** 381 (1956).
8. I. Sakurada and K. Kaji, *Kobunshi Kagaku*, **26,** 817 (1969).
9. J. H. Dumbleton, *J. Polym. Sci. Part A-2*, **6,** 795 (1968).
10. A. J. DeVries, C. Bonnebat, and J. Beautempts, *J. Polym. Sci. Polym. Symp.*, **58,** 109 (1977).
11. H. Takahara and H. Kawai, *Sen i Gakkaishi*, **21,** S235 (1965).
12. D. Patterson and I. M. Ward, *Trans. Faraday Soc.*, **53,** 1516 (1957).
13. M. Kashiwagi, A. Cunningham, A. J. Manuel, and I. M. Ward, *Polymer*, **14,** 111 (1973).
14. I. Kuriyama, K. Tokita, and K. Shirakashi, *Sen i Gakkaishi*, **20,** 431 (1964).
15. J. H. Dumbleton and T. Murayama, *Kolloid-Z. Z. Polym.*, **220,** 41 (1967).
16. T. Kunugi, H. Iwasaki, and M. Hashimoto, *Nippon Kagaku-Kaishi*, **149,** 1981.
17. J. L. Koenig and M. J. Hannon, *J. Macromol. Sci. Phys.*, **B1,** 119 (1967).
18. I. M. Ward, *Structure and Properties of Oriented Polymer*, Applied Science Pub., London, 1975, p. 278.
19. A. Peterlin, *J. Appl. Polym. Sci. Part A-2*, **7,** 1151 (1969).
20. T. Kunugi, A. Suzuki, and M. Hashimoto, *Ashai Garasu Kogyo Gijutsu Shorei-Kai Kenkyu Hokoku*, **36,** 1 (1980).
21. T. Kunugi, I. Akiyama, and M. Hashimoto, *Asahi Garasu Kogyo Gijutsu Shorei-Kai Kenkyu Hokoku*, **36,** 13 (1980).

Received October 15, 1980
Accepted December 11, 1980